Journal of Power Sources 196 (2011) 1171–1177

Contents lists available at ScienceDirect

Journal of Power Sources

journal homepage: www.elsevier.com/locate/jpowsour

Power management system for a 2.5 W remote sensor powered by a sediment microbial fuel cell

Conrad Donovan [b], Alim Dewan [a], Huan Peng [b], Deukhyoun Heo [b], Haluk Beyenal [a,*]

[a] Gene and Linda Voiland School of Chemical Engineering and Bioengineering, Center for Environmental, Sediment and Aquatic Research, Washington State University, Pullman, WA 99163-2710, United States
[b] School of Electrical Engineering and Computer Science, Washington State University, Pullman, WA 99163-2710, United States

ARTICLE INFO

Article history:
Received 3 June 2010
Received in revised form 31 August 2010
Accepted 31 August 2010
Available online 6 September 2010

Keywords:
Microbial fuel cell
Power management
Sediment
Renewable energy
Wireless sensors

ABSTRACT

One of the challenges in using wireless sensors that require high power to monitor the environment is finding a renewable power source that can produce enough power. Sediment microbial fuel cells (SMFCs) are considered an alternative renewable power source for remote monitoring, but current research on SMFCs has demonstrated that they can only produce several to tens of mW of continuous power. This limits the use of SMFCs as an alternative renewable remote power source to mW-level power. Such low power is only enough to operate a low-power sensors. However, there are many remote sensors that require higher power, on the order of watts. Current technology using a SMFC to power a remote sensor requiring watts-level intermittent power is limited because of limitations of power management technology. Our goal was to develop a power management system (PMS) that enables a SMFC to operate a remote sensor consuming 2.5 W of power. We designed a custom PMS to store microbial energy in capacitors and use the stored energy in short bursts. Our results demonstrate that SMFCs can be a viable alternative renewable power source for remote sensors requiring high power.

1. Introduction

Sediment microbial fuel cells (SMFCs) are considered an alternative renewable power source for remote environmental monitoring [1–4]. A SMFC is a device that consists of an anode and a cathode. The anode is buried under the sediment, where there is no oxygen, and the cathode is placed above the sediment, where there is oxygen [1,3,5]. Electrons derived from microbial respiration in the sediments are first accepted at the anode and then transferred through an external circuit to the cathode. The anodic current is usually generated by the oxidation of sedimentary organic carbon, and sulfur compounds [5,6]. The organic compounds in the sediments are oxidized by colonizing bacteria on the anode surface [5]. Sulfate is reduced to sulfide, which is then oxidized to elemental sulfur, transferring the electrons to the anode. The elemental sulfur is oxidized to sulfate in the presence of *Desulfobulbus propionicus* in the sulfur cycle [7]. Literature studies show that sulfate reduction is coupled with organic matter oxidation [7–9]. At the cathode, oxygen is the ultimate electron acceptor.

Most sensors monitoring the environment use either a battery or solar panels as energy sources [10]. The SMFC is an alternative energy source to solar panels. The main advantage of SMFCs over traditional batteries is that they are practically maintenance-free. The main limitations of SMFCs are their low power generation and low output potential [11–13]. To increase the power, researchers have focused on increasing the current by building larger electrodes [14,15], modifying the electrode materials [16–19], and delivering additional fuel to the sediments [20]. On the other hand, the limited output potential of a SMFC cannot be increased by connecting multiple SMFCs in series because all of the electrodes are placed in the same electrolyte solution (water). The output potentials of SMFCs are limited to 300–600 mV, which can be boosted using DC–DC converters for target sensors [1,21]. However, despite efforts to increase the current and potential, the average continuous power from SMFCs is too low to operate remote sensors continuously.

As a solution, the sensors are operated intermittently by storing microbial energy in capacitors and managing the energy using a power management system (PMS) [21]. Recently, our group powered a wireless sensor that consumed 11 mW power, using a SMFC producing an average of 4 mW power [1]. Similarly, Meehan et al. [22] generated 5 mW from a MFC producing 250-μW contin-

* Corresponding author. Tel.: +1 509 335 6607; fax: +1 509 335 4806.
E-mail address: beyenal@wsu.edu (H. Beyenal).

0378-7753/$ – see front matter © 2010 Elsevier B.V. All rights reserved.
doi:10.1016/j.jpowsour.2010.08.099

Nomenclature

C	capacitance (F)
DC/DC	DC to DC converter
DC/DC1	DC to DC converter #1
DC/DC2	DC to DC converter #2
IESC	initial energy storing capacitor
MBR	maximum boost ratio
MFC	microbial fuel cell
P	power (W)
PMS	power management system
P_{avg}	average power (W)
P_{in}	input power (W)
P_{out}	output power (W)
SMFC	sediment microbial fuel cell
TC	transmitter capacitor
TX	transmitter
t_c	time when capacitor is charged (s)
t_d	time when capacitor is discharged (s)
V	potential (V)
V_c	charging potential (V)
V_d	discharging potential (V)
V_{in}	input potential (V)
V_{out}	output potential (V)
W_c	energy stored in the capacitor (J)

uous power [22]. Tender et al. [2] operated two SMFCs in the ocean, producing 24- and 36 mW power. They used the MFCs to operate sensors requiring an average of 18 mW power [2]. The main limitation of all of these systems is that they generate power at the mW level and cannot be used to operate remote environmental sensors that require watt-level power [1,2,21].

Our goal was to develop a power management system that can operate remote sensors requiring high power using a SMFC as a renewable power source. As an example of a sensor requiring high power, we selected a wireless sensor that can transmit data up to 10 miles and requires 2.5 W. We deployed and operated our SMFC in the Palouse River, Pullman, WA, USA. We designed a novel power management system that uses two DC/DC converters and a digital logic circuit to convert low-level power from a SMFC to 2.5 W power.

2. Materials and methods

2.1. Sediment microbial fuel cell

The SMFC was deployed in the Palouse River, Pullman, WA (latitude 46.731°N, longitude −117.178°W, elevation 2352 ft). A sketch of the SMFC used in this study is shown in Fig. 1. The anode was buried in the sediment 0.5 ft below the water–sediment interface. The cathode was placed about 0.5 ft above the water–sediment interface.

2.1.1. The electrodes

The anode was made of a graphite plate (Graphitestore.com, Inc.). It was 30.48 cm × 30.48 cm × 2.54 cm, with a projected surface area of 0.2 m^2. The cathode, which was also made of graphite, had a projected surface area of 1.2 m^2. We used insulated copper wires for electrical connections with both the anode and the cathode. The copper wires were glued to the graphite using conductive epoxy (CW2400, Circuit Works). The connections were covered with silicon rubber to prevent water from contacting the copper wire or the conductive epoxy. The exposure of conductive epoxy to water can cause its corrosion. The wires from the electrodes were about

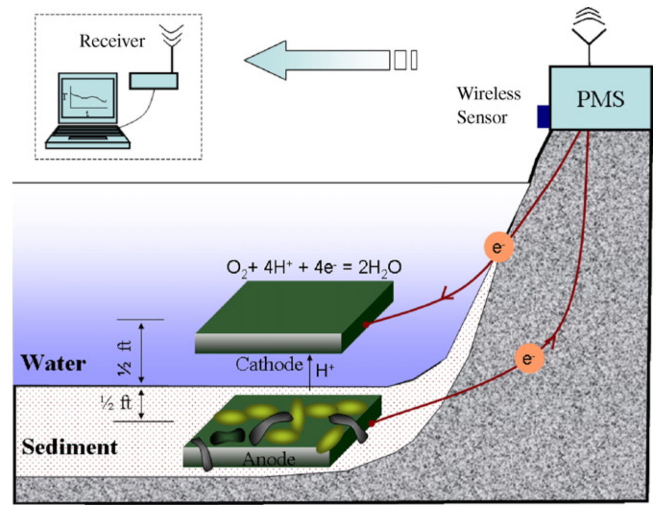

Fig. 1. A sediment microbial fuel cell (SMFC) with microbial anode and cathode provides energy for the power management system (PMS). The graphite electrodes placed under and above the sediment serve as the anode and the cathode, respectively. The PMS stores the energy from the microbial reactions and then converts it to power that is high enough to operate the wireless sensor. The receiver collects the data.

20 ft long, which was long enough to connect to the PMS and the wireless sensor placed by the bank of the river.

2.1.2. Characterization of the SMFC

Initially, the SMFC was run without a load. The open circuit potential (OCP) of the anode and the cathode of the SMFC was measured against a saturated calomel electrode (SCE) using a digital multimeter (Fluke® 189). The power generation of the SMFC was characterized using potentiodynamic polarization with a potentiostat (Reference 600, Gamry Instruments, Inc.) [14]. The power was calculated as the product of the cell potential and the current flowing between the electrodes.

2.1.3. Characterizing long-term power generation of the SMFC

To test the long-term power generation of the SMFC, we used the intermittent energy harvesting method [23]. Intermittent energy harvesting uses the cyclic charging and discharging of a capacitor. Previously, we found that intermittent energy harvesting collects more power from a microbial fuel cell than continuous energy harvesting using a resistor [23]. Since the power management system required a 350 F capacitor to harvest the energy from the SMFC, we characterized the SMFC by cyclically charging and discharging the 350 F capacitor. The capacitor was charged and discharged cyclically from a discharging potential (V_d) of 0 V to a charging potential (V_c) of 500 mV for at least 3 weeks.

The energy (W_c) stored in the capacitor when the capacitor was charged from V_d to V_c was calculated using Eq. (1) [24,25].

$$W_c = \frac{1}{2}C({V_c}^2 - V_d^2) \quad (1)$$

The average power (P_{avg}) generation in a single charging cycle was calculated by dividing the total energy stored in the capacitor by the charging time, as shown in Eq. (2). The charging time ($t_c - t_d$) was calculated by subtracting the time when the capacitor was discharged (t_d) from the time when the capacitor was charged (t_c).

$$P_{avg} = \frac{W_c}{(t_c - t_d)} = \frac{1}{2}\frac{C(V_c^2 - V_d^2)}{(t_c - t_d)} \quad (2)$$

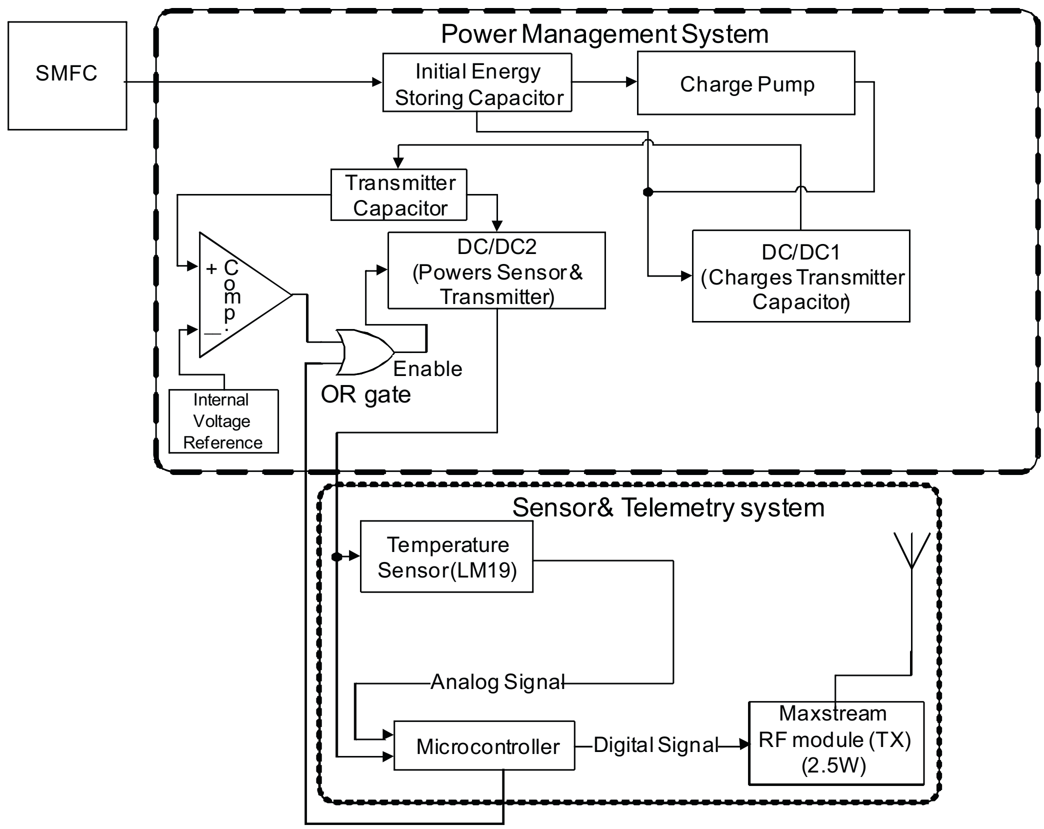

Fig. 2. Block diagram of the PMS, the sensor and the telemetry system.

2.2. Power management system

The custom-designed power management system consisted of energy storing devices (capacitors), a charge pump for automatic repowering of the system, two DC/DC converters, and digital logic to control energy storage and use (Fig. 2).

2.2.1. Initial energy storing capacitor and transmitter capacitor

The energy produced by the SMFC was stored in a capacitor called the initial energy storing capacitor (IESC). This capacitor was connected directly to the SMFC. A 350 F ultracapacitor (Maxwell®) was capable of storing enough energy for sensor operation. The transmitter capacitor (TC) stored energy at a higher potential to be used by the transmitter. The TC was placed after the first DC/DC converter (DC/DC1) and was charged to 4.07 V before the transmission started. We found that a 10 F capacitor was capable of storing enough energy to generate 2.5 W for 5 s, which was enough to operate the sensor and transmit the data.

2.2.2. Determining the size of the capacitors

The size of the capacitors was determined based on the energy requirement of the sensor and telemetry system (Fig. 3). For each measurement by the sensor and data transmission by the telemetry system the rated energy requirement was 1.77 J (Fig. 3). To supply this energy to the sensor and telemetry system, DC/DC2 (80.6% efficiency) drew 2.20 J from the TC. This energy was used to calculate the size of the TC using Eq. (1), with V_c and V_d at 4.07 and 4 V, respectively. The V_c and V_d values were chosen based on the efficient operating potential range of the DC/DC2. We found that a 7.79 F TC was needed to obtain 2.2 J. Since a 7.79 F capacitor was not available the TC was rounded up to 10 F.

The energy supplied to the TC came from the IESC after a loss at DC/DC1. Thus, the energy flow from the IESC was 2.20/0.70 = 3.14 J because DC/DC1 was 70% efficient. The size of the IESC needed to obtain this energy from the SMFC was calculated using Eq. (1). V_c (used in Eq. (1)) was set based on the SMFC potential available under load condition, and V_d was set by the minimum potential of the IESC needed to allow for efficient operation of the system. When a load was applied, the SMFC potential normally varied between 0.3 and 0.4 V. We set V_c to the maximum potential, 0.4 V. V_d was set to 0.375 V to allow the IESC to fluctuate to a maximum of 25 mV. The size of IESC that we calculated was 324 F. We rounded up to 350 F, which was the next size available commercially.

2.2.3. The charge pump and automatic repowering

A charge pump and a feedback circuit were added to the PMS for automatic starting or repowering. We used an ultra-low potential charge pump (S-822Z24). The charge pump jump-starts the DC/DC1 automatically when the IESC accumulates a sufficient energy. Once the system is started, the charge pump is disabled to ensure higher power efficiency of the overall power management system. It then

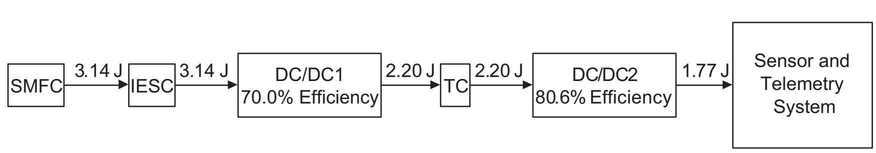

Fig. 3. Energy flow diagram of each transmission of the 2.5 W PMS, which was used to determine the capacitor sizes.

remains disabled until repowering is necessary. We found that a minimum of continuous 3 mW is required to charge the TC. If the power of the SMFC drops below 3 mW, the PMS shuts down. When the SMFC produces more than 3 mW of power again, the charge pump repowers the PMS automatically.

2.2.4. The DC/DC converters

A DC/DC converter is an electronic device which converts a low potential to a higher potential by consuming current. However, a DC/DC converter has a limited ability to increase a low potential to a high potential at which it can operate stably [26]. The boost ratio for a DC/DC converter is defined by the ratio of the input and output potentials. The maximum boost ratio (MBR) is defined as the theoretical highest boost ratio at which a DC/DC converter can operate without the output voltage collapsing; it can be calculated from equations given in the literature [26]. For our 2.5 W system the required boost ratio vary from V_{out}/V_{in} = 5 V/0.3 V = 16.67 to V_{out}/V_{in} = 5 V/0.4 V = 12.5 considering the SMFC potential varies from 0.3 to 0.4. V_{out} is the potential required by the sensor and telemetry system to operate (5 V), and V_{in} is the potential of the SMFC under load (0.3–0.4 V). We calculated theoretical MBR for a single DC/DC converter [26] to be 4.48, which is lower than the required boost ratio (16.67) for our application. Therefore, we used two cascaded DC/DC converters. Given that the output of DC/DC1 was 4.07 V, which was used as the input potential of DC/DC2 to calculate the boost ratio of DC/DC2, with an input potential of 4.07 V, the boost ratio for DC/DC2 is 5 V/4.07 V = 1.23. This ensures that two DC/DC converters will provide the required 2.5 W power.

2.2.5. Digital logic

We designed electronics to control the operation of each DC/DC converter separately. When enough energy accumulated in the IESC, the charge pump jump-started DC/DC1 automatically. DC/DC1 charged the TC to 4.07 V, which triggered the potential comparator to generate a logic high signal to the OR gate. After the logic high signal reached the OR gate, the output of the OR gate changed to logic high, enabling DC/DC2. At that point, the microcontroller was turned on and sent a feedback logic high signal to the OR gate, which ensured that the power would remain on until the microcontroller had successfully sent the serial data to the transmitter and the transmission was successful. Once the transmission was successful, the microcontroller sent a feedback logic low signal to the OR gate, which disabled DC/DC2 and removed power from the sensor and telemetry system.

2.2.6. Calculating the power efficiency of the PMS

The efficiency of the PMS is determined by measuring the power efficiency of the DC/DC converters, assuming that the power consumption by the other components can be ignored. The digital logic, comparator, and temperature sensor bias currents combined are about 30 μA, small enough to ignore. The power efficiency of the charge pump was measured at about 22.5%; however, it only operates during short periods (typically 7 s) when the system is being repowered, so its power consumption is negligible. The power efficiency of a DC/DC converter can be expressed as

$$\eta = 100 \times \frac{P_{out}}{P_{in}} \quad (3)$$

Since DC/DC1 and DC/DC2 are cascaded, the overall system efficiency can be approximated as

$$\eta_{system} = \eta_{DC/DC1} \times \eta_{DC/DC2} \quad (4)$$

2.2.7. Demonstrating the ability of the PMS to deliver 2.5 W

To demonstrate that the PMS could deliver 2.5 W power, we tested the output potential of the PMS with a generic load, a 10-Ω resistor. The resistor was connected after DC/DC2. The potental of the TC and the output potential of DC/DC2 were observed. The power genertion by the PMS was calculated from the equation $P = V^2/R$, where P is power, V is the output potential of DC/DC2, and R is the generic load (10 Ω).

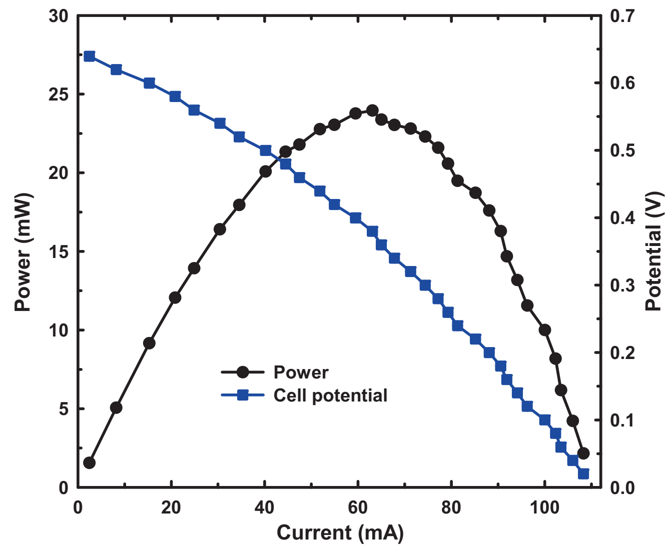

Fig. 4. Characterization of the SMFC. The graphite plate anode (0.2 m^2) was polarized against the graphite plate cathode (1.2 m^2). The scan rate of the polarization was 10 mV s^{-1}.

2.3. The sensor and the telemetry system

The telemetry system consisted of one transmitter and one receiver (brand 9XTend™ OEM) (Fig. 2). The transmitter was operated at 5 V, which was powered by DC/DC2. The transmitter required 2.5 W to operate and transmit the data. The telemetry system was rated at up to 1/3 miles for indoor/urban conditions and up to 10 miles for outdoor line of sight conditions. We used a five-element, 9-dBi yagi (receiving site) and 6″, 2.1-dBi quarter wave whip (transmitting side) antennas. As an example application, we operated a temperature sensor (LM19) which was connected to the telemetry system (Fig. 2). The sensor consisted of a 5 V Freescale microcontroller with an integrated 10-bit analog to digital converter. For each measurement, the sensor microcontroller in the telemetry system took four separate readings at 4-s intervals and averaged them before transmitting. After the temperature readings were logged, the data were sent asynchronously using a serial port on the microcontroller to the buffer in the Maxstream radio modem. From there, the data were transmitted to the receiving radio modem. If needed, the temperature sensor can simply be replaced by any other voltammetric sensor by simply feeding the potential value into the telemetry system.

3. Results and discussions

3.1. Characterization of the SMFC

The cell potential, current and power curves showed that the cell potential decreased linearly with a slope of −0.2 V mA^{-1} when the current was less than 60 mA (Fig. 4). Above 60 mA, the slope decreased to −0.3 V mA^{-1}. This is because of additional potential loss due to mass transfer limitations at high current. We did not observe an activation limitation, which is generally observed at low current as a sharp potential drop [5,27]. Reimers et al. [28] did not see activation limitations in their sediment microbial fuel cell deployed in ocean sediments either [28]. However, Rezaei et al. [3]

observed an activation limitation when they simulated a sediment-based microbial fuel cell in the laboratory. We should note that the current values shown in Fig. 4 are only possible for a very short time. These values are very high compared to what the SMFC can generate during long-term energy harvesting under sustainable conditions [29]. The maximum power was observed when the current and the cell potential were 64 mA and 0.38 V, respectively (Fig. 4), which correspond to a 120 mW m^{-2} power density. Using a similar-sized anode (0.18 m^2) in ocean sediment, Tender et al. [5] observed a 28 mW m^{-2} maximum power density. Similarly, in our previous study, we used the same sizes of anode and cathode and observed a 24 mW m^{-2} maximum power density [1]. We should note again that these studies used different polarization techniques and conditions, which makes it difficult to compare the values. We used a potentiostat with a 10 mV s^{-1} scan rate for our polarization experiments. We observed that the power generation varies significantly depending on the scan rate. In our previous study (in which we were not able to use a potentiostat) we characterized the SMFC using a resistor scan in which each resistor was scanned for 30 s [1]. Therefore, we conclude that the power estimated from a resistor or potentiostat scan is only useful for identifying the factors limiting the power generation, not for actually comparing power between microbial fuel cells. For example, in this study we found that at low current (0–60 mA) the power generation is limited by the ohmic resistance of the electrolyte (Fig. 4). On the other hand, Dumas et al. [13] and Scott et al. [30] observed that at low current densities the power generation is limited by the activation resistances of the electrode reaction.

Since the power estimated from polarization experiments provides information only about the controlling factors of the power generation and cannot be used as the steady state power of SMFC, we estimated the steady state power from our SMFC using intermittent energy harvesting [23,25]. Using a 350 F capacitor we found that the sustainable power produced by our SMFC was 3.4 mW, giving a power density of 17 mW m^{-2}. In the ocean cold seep, Reimers et al. [28] observed a maximum power density of 34 mW m^{-2} during the 20–31st days of operation and a decrease in maximum power density to 6 mW m^{-2} during the 103–114th days of operation [28]. Dumas et al. [13] also observed power generation comparable with that of our SMFC. They deployed a microbial fuel cell in the Mediterranean Sea (Italy) [13] and found that after continuous operation for 17 days their cell produced 4 mW m^{-2}.

3.2. Energy harvesting from the SMFC

Energy was harvested from the SMFC using a 350 F capacitor as the initial energy storing capacitor (IESC). Fig. 5 shows an example of charging and discharging of the capacitor. Charging the capacitor from 0 to 0.5 V took an average of 3.54 ± 0.06 h (Fig. 5). In studies similar to ours, Shantaram et al. [21] charged a 4 F capacitor from 0 to 0.5 V in 2 min using a microbial fuel cell with a sacrificial anode and Donovan et al. [1] charged a 10 F capacitor in 10 min. Our capacitor size was 35 times larger than the capacitor used by Donovan et al. [1]. Using a linear correlation, a 10 F capacitor should be charged by our SMFC in 6.12 min. This time is comparable with the charging time observed by Donovan et al. [1]. We should note that this is the first time we have demonstrated that a SMFC can charge such a large capacitor, which actually allows us to store significant energy and generate high power from a SMFC.

3.3. Demonstration that the PMS can deliver 2.5 W

Fig. 6 shows the DC/DC2 output potential during power generation under a generic load (10-Ω resistor). The output potential of DC/DC2 remained stable around 5 V (161.5 to 166.5 s). This demonstrates that the PMS was able to generate 2.5 W

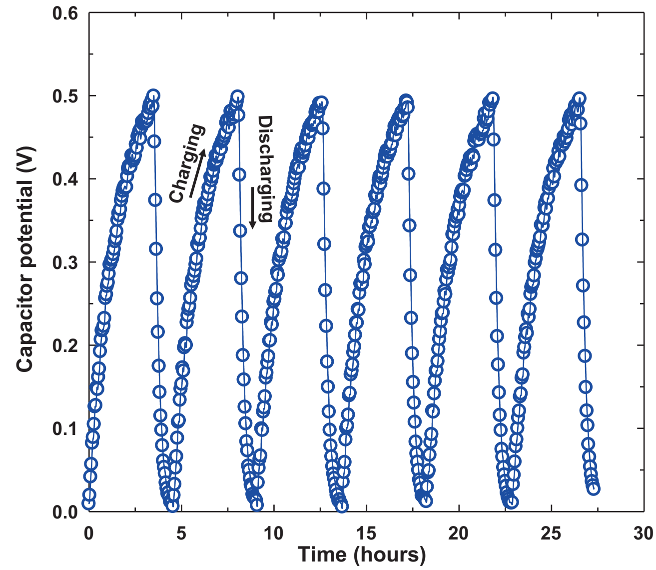

Fig. 5. Example 350 F capacitor charging and discharging curve obtained using the SMFC deployed in the Palouse River.

($P = V^2/R = 5^2/10 = 2.5$ W). The PMS could handle 10-Ω load for approximately 5 s before the potential dropped significantly. Five seconds is enough to perform a measurement and transmit the data. After transmission, DC/DC2 shut down completely when the output potential from DC/DC2 dropped below 4 V; however, charging of the 10 F capacitor continued.

3.4. Data transmission by the PMS

Fig. 7 shows the TC and IESC potential profile during the startup and data transmission by the 2.5 W telemetry system. The potential of the IESC was 0 V before it is was connected to the SMFC. Once it was connected, the potential started to rise. When the potential of the IESC reached 320 mV, the charge pump was activated, which jump-started DC/DC1 automatically. DC/DC1 in turn began to charge the TC (Fig. 7). Since DC/DC1 was drawing additional

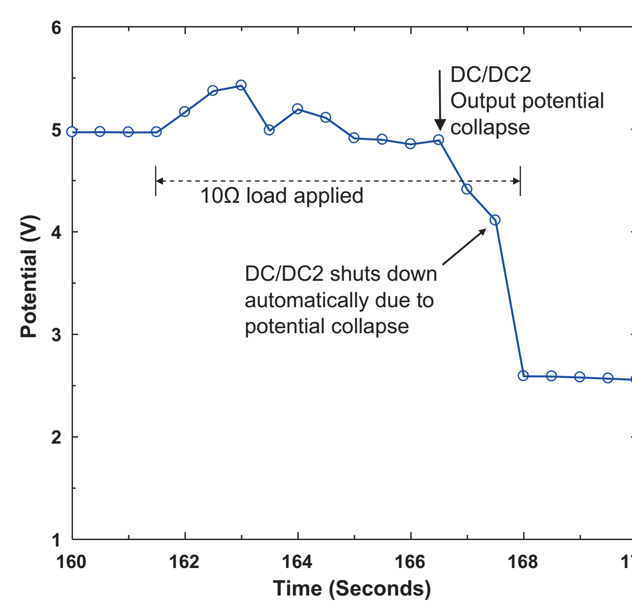

Fig. 6. The DC/DC2 output potential when a 10-Ω load was applied after the DC/DC2 converter.

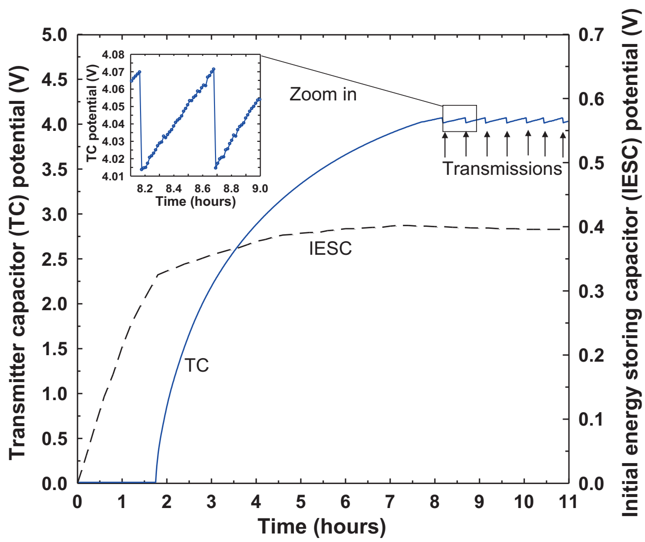

Fig. 7. Transmitter capacitor and initial energy storing capacitor potential during startup and data transmission. Inset: close up of TC potential during a transmission cycle.

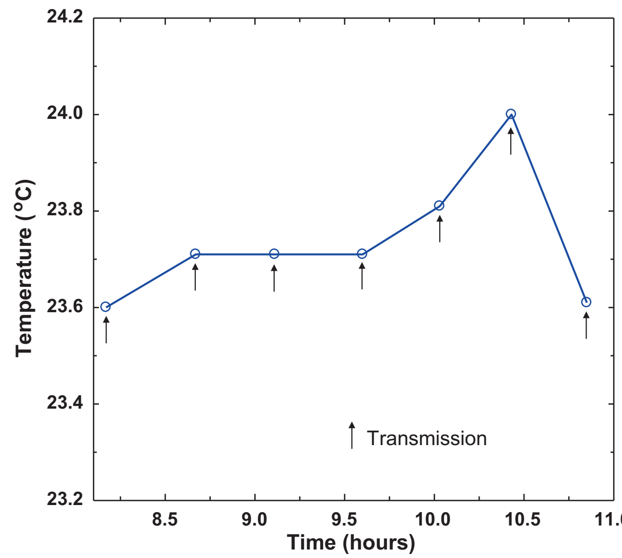

Fig. 8. Temperature data read by the wireless sensor that was powered by the SMFC.

power from the SMFC, the IESC began to charge at a slower rate and eventually settled around 395 mV. The IESC potential fluctuated 3–5 mV during each transmission. After DC/DC1 started, the charge pump was deactivated and the potential on the TC continued to rise until it reached 4.07 V (inset, Fig. 7), which was enough to activate DC/DC2 and start the data transmission (Fig. 7). Once the TC potential reached 4.07 V, the potential comparator sent a signal to the digital logic circuit, which then sent a signal to DC/DC2 to power up the sensor and telemetry system. Once the temperature sensor collected the data, the signal was sent to the transmitter. The transmitter typically consumed 2.5 W during each transmission, which caused the potential of the TC to drop to 4.015 V (inset, Fig. 7). The transmissions were 27 ± 2.4 min apart, which gave DC/DC1 the time needed to charge the TC to 4.07 V. Once transmission started, the potential of the TC decreased from 4.070 to 4.015 V.

3.5. Example temperature measurement using a wireless sensor powered by the SMFC

Fig. 8 shows representative temperature data measured using the developed PMS, and the temperature sensor and telemetry system powered by the SMFC deployed in the Palouse River. The sensor measured the ambient temperature near the river. The time interval between data transmissions was 27 ± 2.4 min on average. This time interval can be decreased if the power generation by the SMFC is increased. We found that the time interval fluctuates over time due to variation in power generation by the SMFC.

3.6. Power efficiency of the PMS

Fig. 9 shows the power efficiency of DC/DC1 with a SMFC input potential of 395 mV. When DC/DC1 was operated with an output current of about 1 mA the efficiency was 70.0%. The power efficiency of DC/DC2 (Fig. 9) was 80.6% with an input potential of 4.07 V and an output current of 500 mA. Thus, the overall system efficiency under these operating conditions was 70.0% × 80.6% = 56.4%. Since, practically the power from SMFC would vary with the environmental conditions such as rain or temperature, we also tested efficiency of power management system under simulated non-rhythmic conditions. A variable series resistance was placed between the SMFC and the PMS to simulate non-rhythmic charge–discharge cycles. We found that the power efficiency did not change.

3.7. Application of the developed PMS to other wireless sensors

The developed SMFC and PMS can be used to power other sensors requiring 2.5 W or less power. For example, we could power light-dependent resistors (LDR), light-emitting diodes (LED), laser diodes or metal oxide or pH electrodes, which consume 250, 225, 280 and 60 mW, respectively [10]. These power consumptions will vary depending on the type of telemetry system used.

Our study demonstrates that SMFC can be used to generate power much higher than the mW levels of previously available. The SMFC and customized PMS can use approximately 3.4 mW continuous average power, store it in a capacitor and then generate 2.5 W power for a maximum of 5 s for each charging cycle. The developed system can be customized to monitor environments more frequently while transmitting the measured data over longer distances. We believe that the developed novel concepts of integrating

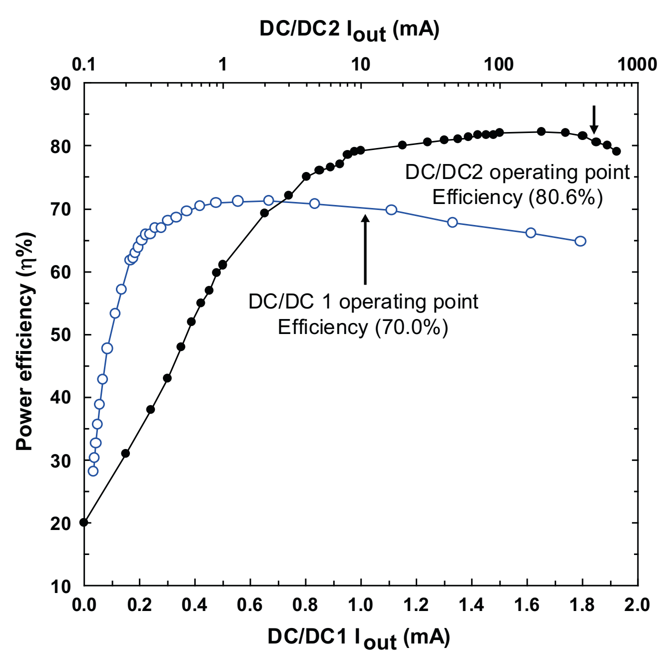

Fig. 9. Power efficiency versus output current for DC/DC1 with V_{in} = 395 mV and V_{out} = 4.07 V and for DC/DC2 with V_{in} = 4 V and V_{out} = 5 V.

the SMFC, the electronic system and the designed PMS can be used for remote enviroment monitoring.

4. Conclusions

- A SMFC producing 3.4 mW average continuous power produce 2.5 W power intermittently, and this power can be used to operate a wireless sensor.
- A SMFC can be used as a renewable alternative power source for remote sensors requiring high power.

Acknowledgements

The authors would like to thank the Gene and Linda Voiland School of Chemical Engineering and Bioengineering for startup funds in support of the research (Dr. Beyenal). The authors gratefully acknowledge the financial support provided by 3M, NSF IGERT (DGE-0900781) for Conrad Donavan, and NSF (ECCS-0845849) for Huan Peng. The authors also acknowledge Nghia Tang for his technical discussion.

References

[1] C. Donovan, A. Dewan, D. Heo, H. Beyenal, Batteryless, Environ. Sci. Technol. 42 (2008) 8591–8596.
[2] L.M. Tender, S.A. Gray, E. Groveman, D.A. Lowy, P. Kauffman, J. Melhado, R.C. Tyce, D. Flynn, R. Petrecca, J. Dobarro, J. Power Sources 179 (2008) 571–575.
[3] F. Rezaei, T.L. Richard, R.A. Brennan, B.E. Logan, Substrate-enhanced microbial fuel cells for improved remote power generation from sediment-based systems, Environ. Sci. Technol. 41 (2007) 4053–4058.
[4] Z. He, H. Shao, L.T. Angenent, Biosens. Bioelectron. 22 (2007) 3252–3255.
[5] L.M. Tender, C.E. Reimers, H.A. Stecher, D.E. Holmes, D.R. Bond, D.A. Lowy, K. Pilobello, S.J. Fertig, D.R. Lovley, Nat. Biotechnol. 20 (2002) 821–825.
[6] C.E. Reimers, L.M. Tender, S. Fertig, W. Wang, Environ. Sci. Technol. 35 (2001) 192–195.
[7] D.E. Holmes, D.R. Bond, R.A. O'Neill, C.E. Reimers, L.R. Tender, D.R. Lovley, Microb. Ecol. 48 (2004) 178–190.
[8] N. Ryckelynck, H.A. Stecher, C.E. Reimers, Biogeochemistry 76 (2005) 113–139.
[9] D.E. Holmes, D.R. Bond, D.R. Lovley, Appl. Environ. Microbiol. 70 (2004) 1234–1237.
[10] D. Diamond, S. Coyle, S. Scarmagnani, J. Hayes, Chem. Rev. 108 (2008) 652–679.
[11] M.E. Nielsen, C.E. Reimers, H.A. Stecher, Environ. Sci. Technol. 41 (2007) 7895–7900.
[12] M.E. Nielsen, C.E. Reimers, H.K. White, S. Sharma, P.R. Girguis, Energy Environ. Sci. 1 (2008) 584–593.
[13] C. Dumas, A. Mollica, D. Feron, R. Basseguy, L. Etcheverry, A. Bergel, Electrochim. Acta 53 (2007) 468–473.
[14] A. Dewan, H. Beyenal, Z. Lewandowski, Environ. Sci. Technol. 42 (2008) 7643–7648.
[15] B.E. Logan, Appl. Microb. Biotechnol. 85 (2010) 1665–1671.
[16] S. Cheng, H. Liu, B.E. Logan, Environ. Sci. Technol. 40 (2006) 364–369.
[17] O. Lefebvre, W.K. Ooi, Z. Tang, M. Abdullah-Al-Mamun, D.H.C. Chua, H.Y. Ng, Bioresource Technol. 100 (2009) 4907–4910.
[18] P. Aelterman, M. Versichele, E. Genettello, K. Verbeken, W. Verstraete, Electrochim. Acta 54 (2009) 5754–5760.
[19] S. You, Q. Zhao, J. Zhang, J. Jiang, C. Wan, M. Du, S. Zhao, J. Power Sources 173 (2007) 172–177.
[20] M.E. Nielsen, D.M. Wu, P.R. Girguis, C.E. Reimers, Environ. Sci. Technol. 43 (2009) 8671–8677.
[21] A. Shantaram, H. Beyenal, R. Raajan, A. Veluchamy, Z. Lewandowski, Environ. Sci. Technol. 39 (2005) 5037–5042.
[22] A. Meehan, H. Gao, Z. Lewandowski, IEEE Energy Conversion Congress Exposition (2009) 3558–3563, Article no. 5316034.
[23] A. Dewan, H. Beyenal, Z. Lewandowski, Environ. Sci. Technol. 43 (2009) 4600–4605.
[24] J.R. Cogdell, Foundations of Electric Circuits, Pearson Custom Publishing, 1999.
[25] A. Dewan, C. Donovan, D. Heo, H Beyenal, J. Power Sources 195 (2010) 90–96.
[26] H. Mahmood, K. Natarajan, IEEE (2008) 273–278.
[27] S.H. Shin, Y.J. Choi, S.H. Na, S.H. Jung, S. Kim, Bull. Korean Chem. Soc. 27 (2006) 281–285.
[28] C.E. Reimers, P. Girguis, H.A. Stecher III, L.M. Tender, N. Ryckelynck, Geobiology 4 (2006) 123–136.
[29] J. Menicucci, H. Beyenal, E. Marsili, R.A. Veluchamy, G. Demir, Z. Lewandowski, Environ. Sci. Technol. 40 (2006) 1062–1068.
[30] K. Scott, I. Cotlarciuc, I. Head, K.P. Katuri, D. Hall, J.B. Lakeman, D. Browning, Fuel cell power generation from marine sediments: Investigation of cathode materials, Journal of Chemical Technology and Biotechnology 83 (2008) 1244–1254.